International Journal of Microwave and Wireless Technologies

cambridge.org/mrf

Design of subwavelength metamaterial resonator based on new self-coupling strategy

Larbi Benkhaoua[1,2], Smail Mouissat[1], Mohamed Taoufik Benhabiles[1] and Mohamed Lahdi Riabi[1]

[1]Université des Frères Mentouri, Constantine, Algeria and [2]Université 8 Mai 1945, Guelma, Algeria

Research Paper

Cite this article: Benkhaoua L, Mouissat S, Benhabiles MT, Riabi ML (2020). Design of subwavelength metamaterial resonator based on new self-coupling strategy. *International Journal of Microwave and Wireless Technologies* **12**, 221–226. https://doi.org/10.1017/S1759078719001259

Received: 25 January 2019
Revised: 23 August 2019
Accepted: 29 August 2019
First published online: 20 September 2019

Key words:
Device miniaturization; metamaterial resonators; self-coupling; split-ring resonator (SRR)

Author for correspondence:
Larbi Benkhaoua,
E-mail: benkhaoua.alarbi@umc.edu.dz

Abstract

In this paper, edge-broad-side coupled spiral resonator (EBC-SR) is proposed to enhance the miniaturization of the metamaterial resonators. After a comparative analysis, it is found that the proposed strategy can drastically reduce the electrical size of metamaterial resonators. This is due to the use, at the same time, advantages of edge coupling, broad-side coupling, and self-coupling. A lumped element equivalent circuit model is proposed for the EBC-SR-loaded transmission line. This model is validated by comparing the results of electromagnetic simulations with the circuit simulations using the extracted parameter values. To validate the proposed strategy, a prototype of the EBC-SR embedded inside a drive loop is fabricated. The experimental results are presented with the simulation results.

Introduction

Since the first realization of the magnetic structure (metamaterial resonator) proposed by Pendry [1], negative values of permeability can be obtained in a narrow band above resonance. This particle called the edge-coupled split-ring resonator (EC-SRR). In the literature, there are many alternatives to EC-SRR. Due to their small electrical size, this kind of planar resonators can be employed in many different microwave devices such as the design of left-handed transmission lines [2]. Usually, these miniaturized resonators are excited by magnetic [2] or electric fields [3] of transmission lines (microstrip lines or coplanar waveguides (CPW)) to allow a strong coupling in compact configurations. To achieve the miniaturization required by many applications such as small electronic devices and implanted medical devices, the electrical size of the metamaterial resonator should be kept as small as possible. For this reason, one of the main scientific objectives in this research field is focused on the development of sub-wavelength inclusions to achieve a smaller electrical size. Some famous resonators based on different configurations were developed, and may represent a topical state of the art for our work.

In [1], the authors proposed the EC-SRR constituted by two concentric split rings designed in order to interchange the effective energy between the individual rings. This resonator can be modeled by an equivalent inductance L_s and a capacitance C_s in the form of a series resonant circuit. Specifically, the rings form the inductance and the regions between the strips form the capacitance [4]. The resonance frequency takes place when the electric energy stored in the capacitance is balanced with the magnetic energy stored in the inductance, consequently this resonance is proportional to $(L_s\ C_s)^{-1/2}$. In [5], the authors demonstrated that the two winds spiral resonator (SR) is able to reduce the electrical size by a factor of 1/2 compared to the EC-SRR. In [6] and [7], another strategy for the miniaturization is presented. It is based on the increasing of the inductance of EC-SRR by the augmentation of the number of rings. The results particle is called multiple-SRR (M-SRR). In [8], the broad-side strategy is introduced by etching the two rings of the EC-SRR at both sides of the substrate, face-to-face in the anti-parallel fashion as broad-side coupled split-ring resonator (BC-SRR). In this case, the electrical size of the resonator becomes much smaller due to enhanced capacitance between the two metal layers, particularly if a thin substrate is used. In [9], the authors showed that more size reduction can also be reached by replacing the individual rings of the BC-SRR by M-SRR or SR. these particles can be called double-sided M-SRR (DM-SRR), and double-sided SR (D-SR), respectively. Generally the use of broad-side topologies provides much smaller electrical sizes compared to the single-sided topologies. In [10], a self-coupling broad-side coupled spiral resonator (BC-SR) is proposed. In this particle, the SRs in the two metal layers are connected by a via. This association increases the inductance and the distributed capacitance of the resonator. As a consequence, the electrical size of the resonator was significantly reduced compared to all resonators mentioned above. At the fundamental resonance, each metal layer has only one type of electric charge (positive or negative) due to the extended strips through via. Hence the BC-SR does not contain any edge coupling due to the absence of edge

© Cambridge University Press and the European Microwave Association 2019

CAMBRIDGE UNIVERSITY PRESS

capacitances; consequently the coupling mechanism is mainly governed by the broad-side capacitance between the two metal layers.

In [11], after a detailed comparative analysis of different topologies, the authors concluded that the use of metallic vias in the case of the BC-SR does not represent a severe degradation in the quality factor of resonators. For this last reason, in the present study, we did not interest to the quality factor of resonators.

We should also mention that other approaches for miniaturization are proposed in the literature. They are based on the use of: lumped capacitance loaded loop [12], embedded high dielectric constant paste on the top of a conventional resonator [13], superconducting thin film [14], ferrite loaded solenoid [15], and insulator layer between metal layers [16]. In the present work, we focalized only on the metamaterial resonators that can be fabricated by the conventionals printed circuit board manufacturing techniques.

In this paper to enhance the miniaturization of metamaterial resonators, a new kind of self-coupling resonator is proposed using at the same time the effects of broad-side coupling and edge coupling. To the best of our knowledge, this is the first study that uses simultaneously the effects of the broad-side coupling, the edge coupling, and the self-coupling to design a metamaterial resonator.

Design

The proposed resonator that can be called the edge-broad-side coupled spiral resonator (EBC-SR) is presented in Fig. 1. Its geometry is particularly designed to enlarge the broadside coupling and the edge coupling together by etching two parallel winding SRs at each side of the substrate, and connected them through three metallic vias to have a full connected metallic strip along the whole structure. The electrical size of this resonator can be significantly reduced compared to the existing metamaterial resonators. This is due to the simultaneous presence of the: (a) high inductance of the extended strips due to the self-coupling by using vias. (b) Broad-side capacitance C_{BC} between the two metallic layers due to the broadside coupling. (c) Edge capacitance C_{EC} due to the edge coupling. We should mention that, the proposed resonator and the BC-SR have the same inductance and broad-side capacitance C_{BC}, but contrary to the proposed resonator, the BC-SR does not contain any edge coupling. The miniaturization property of our resonator arises from the presence of the edge capacitance C_{EC} distributed between each two adjacent metallic turns, on both substrate sides, due to the edge coupling. To points up the distributed capacitances C_{BC} and C_{EC}, Fig. 1 illustrates the distribution of charges at the resonance frequency of the EBC-SR with six turns (three turns on both substrate sides).

The proposed resonator (EBC-SR) is inspired mainly from the original SRR topology proposed by Pendry [1]. Then, it essentially behaves as a capacitive load conducting loop which gives a resonant behavior. It therefore exhibits a diamagnetic behavior near the resonance frequency for the external time-varying magnetic field polarized in the axial direction (so the EBC-SR is a magnetically coupled resonator) [17]. Hence, the EBC-SR is expected to exhibit a negative effective permeability in a certain band of frequencies as a small metamaterial resonator.

In the following sections, a comparative study is provided to show the advantages of the proposed resonator over existing metamaterial resonators. It is carried out with numerical simulations using High-Frequency Structure Simulator (HFSS) commercial software of Ansoft Corporation. Its frequency domain electromagnetic solver is based on the Finite Element Method (FEM).

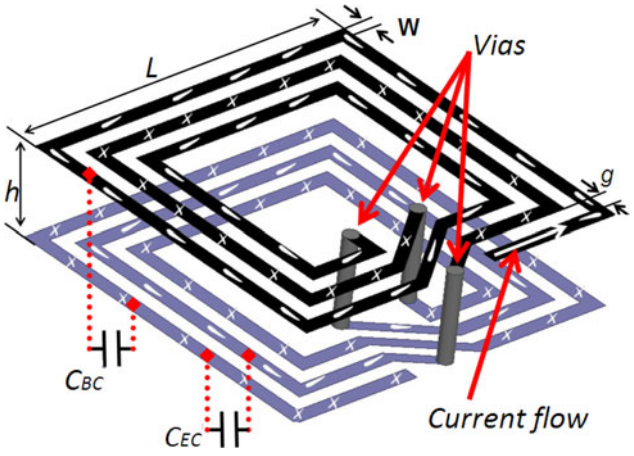


Fig. 1. Topology of the EBC-SR with three turns on both substrate sides and distribution of charges at the fundamental resonance.

Figure 2 shows the simulated transmission scattering parameter S_{21} of the EBC-SR with two turns on both substrate sides. For comparison, Fig. 2 also includes the frequency responses of the EC-SRR [1], the SR [5], the BC-SRR [8], and the BC-SR [10] (Fig. 3). In the first time, to get the transmission coefficient S_{21}, the different resonators are excited by a plane wave. The resonance frequency is revealed by a notch in the transmission coefficient. The dimensions and the substrate used in all these structures are chosen to be identical. The width of the metallic strips is $w = 0.4$ mm, the gap width between adjacent strips is $g = 0.4$ mm, the side length is $L = 20.4$ mm, and the substrate used is duroid5880, which has a dielectric constant ε_r of 2.2, loss tangent of 0.0009, and thickness $h = 0.79$ mm (Fig. 1).

To give an idea about the magnetic behavior of the particle, Fig. 4 shows the inspection of the surface current distribution in the resonator inferred from HFSS. It reveals that at resonance the rotation direction of the current flow remains the same in all turns of the EBC-SR. Hence, there is no current cancellation in this resonator and no destructive interferences between the magnetic fields formed by the currents in the rings at both sides of the substrate. This characteristic is of great interest for the synthesis of metamaterials, and in general, for any application requiring magnetically coupled resonators [11].

The electrical size U of the resonators is defined as:

$$U = \frac{D}{\lambda_0}, \tag{1}$$

where D is the maximum linear dimension of the resonator and λ_0 is the wavelength at resonance frequency f_0.

Table 1 summarizes the values of the resonance frequency and the electrical size of different metamaterial resonators by applying formula (1) on the numerical simulation results of Fig. 2. The electrical size is identified in terms of λ_0 as in [6]. We show clearly that the EBC-SR is the electrically smaller resonator with $U = \lambda_0/73$ and $f_0 = 141.7$ MHz.

We should note that, for two turns on both substrate sides, the resonance frequency f_0 in the case of the EBC-SR is lower than that of the BC-SR having the same number of turns by 12.26%.

https://doi.org/10.1017/S1759078719001259 Published online by Cambridge University Press

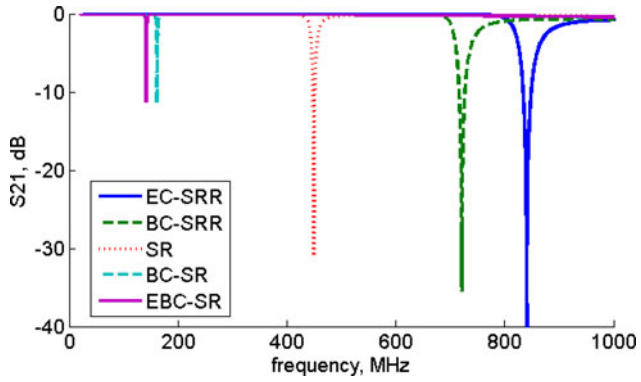


Fig. 2. Simulated transmission scattering parameter S_{21} of the EBC-SR, EC-SRR, SR, BC-SRR, and BC-SR (the dimensions and the substrate used in all these structures are chosen to be identical).

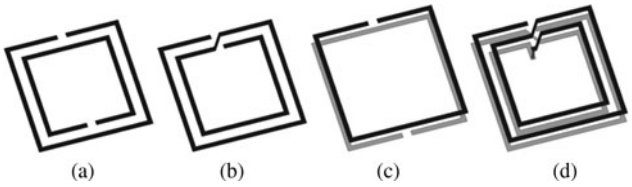


Fig. 3. Structures of (a) EC-SRR, (b) SR, (c) BC-SRR, and (d) BC-SR.

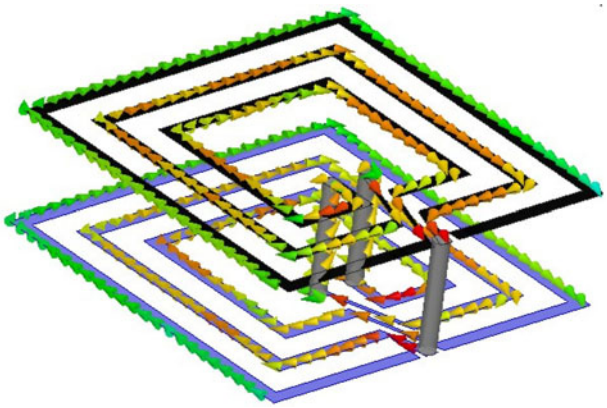


Fig. 4. Sketch of the surface current distributions in the resonator inferred from the simulation at the fundamental resonance.

This difference points out the effect of the edge capacitances C_{EC} distributed between the metallic turns of the EBC-SR.

The EBC-SR can achieve more miniaturization by increasing the turns number. In this case, the C_{EC} becomes the dominant coupling mechanism at the resonance of the EBC-SR compared to its lack in the BC-SR, having the same turns number. Figure 5 shows the EBC-SR and BC-SR behaviors as a function of the number of turns N at each side of the substrate. The values of the resonance frequency and the electrical size of the EBC-SR, BC-SR, and SR are summarized in Table 2 for N equals 2, 4, 6, 8, and 10. For the three resonators, as we increase the number of turns, the resonance frequency shifts to lower values. This can be explained by the changes in the total inductance L_s and the capacitance C_s of the resonators. We show also that, by increasing

Table 1. Comparison between EBC-SR and different resonators in terms of resonance frequency and electrical size U

Topology	f_0 (MHz)	$U(\lambda_0)$
EC-SRR	840.5	1/12
BC-SRR	721.2	1/14
SR	449.3	1/23
BC-SR	161.5	1/64
EBC-SR	141.7	1/73

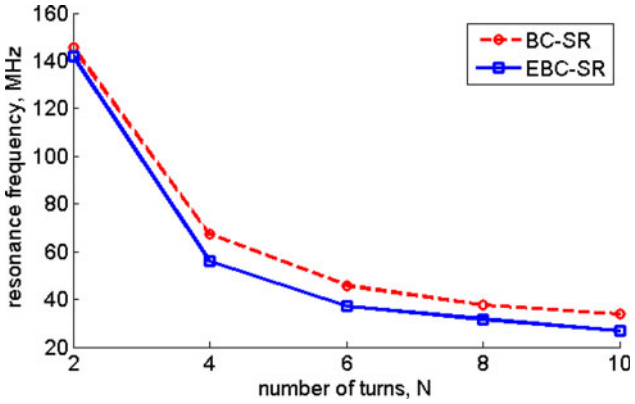


Fig. 5. Resonance frequency of EBC-SR and BC-SR as a function of the number of turns at each side of the substrate.

N, the effect of the distributed capacitance C_{EC} of the EBC-SR becomes more significant. As an example, for $N = 10$ the resonance frequency f_0 of the EBC-SR is lower than that of the BC-SR by 20.71%, which is more important than that shown in the case of $N = 2$, that is only 12.26%.

By means of an electromagnetic simulator, the resonance frequency can be adjusted by changing the dimensions of the proposed resonator to accurately meet the desired frequency.

The EBC-SR can be excited by the axial time-varying magnetic field of a microstrip line or CPW, which exhibits a stopband in the vicinity of the fundamental resonance frequency. Compared to the microstrip line configuration, the magnetic field lines penetrate efficiently the EBC-SR area and a higher magnetic coupling is achieved by placing on the back side of the substrate of CPW a pair of resonators, their centers located under the two slots of the CPW Fig. 6.

According to [18], the EBC-SR-loaded CPW can be modeled by the lumped-element equivalent circuits shown in Fig. 7(a). Where L and C are the per-section inductance and capacitance of the CPW line, the resonators are described by the resonant tank L_s-C_s, and the mutual magnetic coupling between the line and the resonators is represented by M. This model can be changed to the model depicted in Fig. 7(b), where:

$$L'_s = 2M^2 C_s \omega_0^2, \tag{2}$$

$$C'_s = L_s / 2M^2 \omega_0^2, \tag{3}$$

$$L' = L - L'_s. \tag{4}$$

https://doi.org/10.1017/S1759078719001259 Published online by Cambridge University Press

Table 2. Resonance frequency and electrical size of EBC-SR, BC-SR and SR as a function of the number of turns at each substrate side

N	SR f_0 (MHz) – $U(\lambda_0)$	BC-SR f_0 (MHz) – $U(\lambda_0)$	EBC-SR f_0 (MHz) – $U(\lambda_0)$
2	449.3–1/23	161.5–1/64	141.7–1/73
4	245.7–1/42	67.1 –1/155	56.0–1/185
6	203.6–1/51	45.8–1/227	37.2–1/279
8	181.4 –1/57	37.5–1/277	31.7–1/328
10	178.9– 1/58	33.8–1/308	26.8–1/388

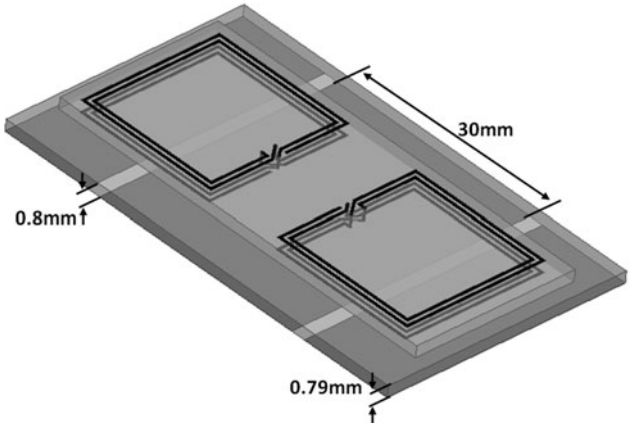


Fig. 6. Topology of the CPW loaded with a pair of EBC-SR with two turns on both substrate sides.

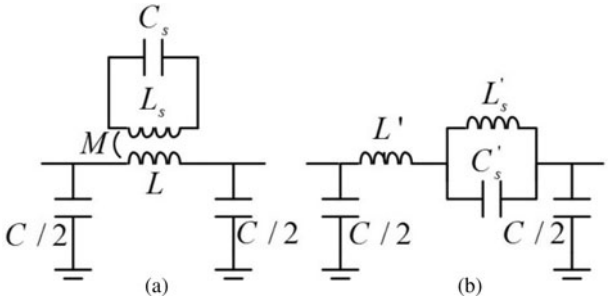


Fig. 7. Lumped element equivalent circuit model of the EBC-SR-loaded CPW (a) and transformed model (b).

Hence, the resonance frequency of this structure coincides with the intrinsic resonance frequency of the EBC-SR formed by L_s and C_s and given by:

$$f_0 = \frac{1}{2\pi\sqrt{L'_s C'_s}} = \frac{1}{2\pi\sqrt{L_s C_s}}. \quad (5)$$

At this frequency, the series branch opens and the transmission coefficient exhibits a transmission zero.

To validate the circuit model and to compare the frequency response of the proposed resonator and the BC-SR when they are coupled to the CPW as in Fig. 6, electromagnetic simulations are carried out. The parameter values of the equivalent circuit are obtained by using the procedure explained in [18]. The extracted

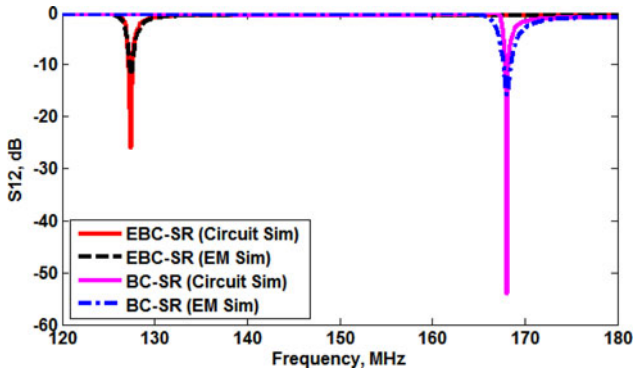


Fig. 8. Transmission scattering parameter S_{21} of the EBC-SR-loaded CPW and the BC-SR-loaded CPW given by numerical simulations and electrical simulations.

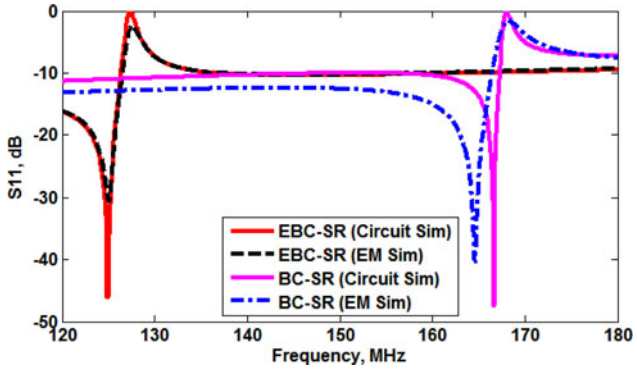


Fig. 9. Reflection scattering parameter S_{11} of the EBC-SR-loaded CPW and the BC-SR-loaded CPW given by numerical simulations and electrical simulations.

parameters for the EBC-SR case are found to be: $C = 16.012$ pF, $L' = 8.45$ nH, $C'_s = 1.435$ nF, and $L'_s = 1.087$ nH. The results of the electrical simulations of the circuit model using the extracted parameter values are depicted in Figs 8 and 9. Good agreement is shown between the frequency response of the circuit simulations and the electromagnetic simulations. Hence, the circuit model is validated. We can see that the resonance frequency f_0 of the EBC-SR is still lower than that of the BC-SR having the same turns number (two turns on both substrate sides). It should be taken into account that the EBC-SR losses due to the presence of three metallic vias provide slight degradation in the *Q*-factor and the notch depth in S_{21} (Fig. 8).

For the proposed resonator with two metal layers, four metal layers are necessary: two for the resonator and two for the microstrip line (in the case of the EBC-SR-loaded CPW, three metal layers are necessary: two for the resonator and one for the host line) which is difficult to fabricate and assemble this particle with other planar devices as all broad-side resonators. Note that as an alternative, a drive loop can be used instead of the transmission line as in [19] which allow a compact structure.

Last but not least, to validate the proposed strategy, an EBC-SR for *N* equals 10 has been fabricated using the above mentioned dimensions with a tolerance of 10%. The insert in Fig. 10 shows the photograph of the fabricated prototype. The EBC-SR is placed in the interior of a drive loop in order to excite it in the axial direction with an intense external time-varying magnetic field. The reflection coefficient S_{11} of the fabricated prototype is measured using a vector network analyzer (VNA). The

https://doi.org/10.1017/S1759078719001259 Published online by Cambridge University Press

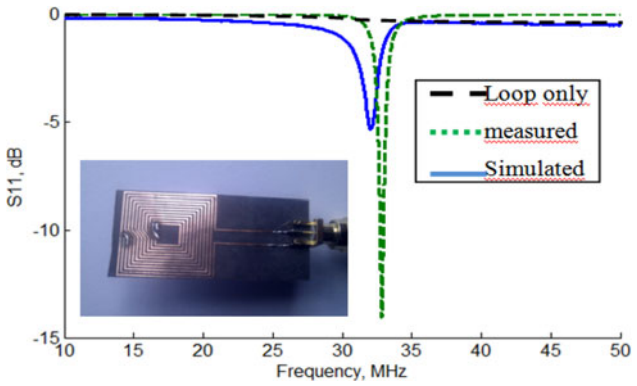


Fig. 10. Simulated and measured reflection scattering parameter S_{11} of the fabricated prototype.

comparison between the measured and simulated S_{11} is shown in Fig. 10. We observe a small difference in the resonant frequency; due to both HFSS discrepancies with real-world setups, and the fabrication tolerance limits.

We should mention that, due to the electromagnetic signal generated in the VNA (and received by the EBC-SR through magnetic coupling), an electromotive force (emf) is induced in the EBC-SR. This emf reaches a maximum at f_0, which in turn generates a back-emf across the drive loop. Therefore, at resonance, the magnitude of the reflected voltage is minimum, which appears as a notch in the reflection coefficient curve S_{11} [19]. Hence this notch is the direct consequence of the radiated energy by the EBC-SR at the resonance frequency. We can see from the simulated response of the drive loop only in Fig. 10 that this latter is non-resonating.

We would like to mention that further shift down of the EBC-SR resonance frequency can be realized by using a higher permittivity substrate ε_r due to the dependence of ε_r with the broad-side capacitance C_{BC} and the edge capacitance C_{EC}.

This kind of resonators will be an excellent candidate for many RF/microwave applications as implanted medical devices; in particular, we can use it as miniaturized receiving coils of Planar Magnetically Coupled Resonant Wireless Power Transfer Systems (MCR-WPT) as in [20–21], or use it as unit cell for designing metamaterial transmission lines as in [18].

Conclusion

The miniaturization potential of the proposed strategy has been demonstrated by a comparative analysis of the EBC-SR with different metamaterial resonators. We have also validated the circuit models describing the EBC-SR-loaded transmission lines. It has been shown that the proposed EBC-SR provides a miniaturization factor less than that of a BC-SR having the same turns number; 10 turns, by 20.71%, which make it a practical candidate for the receiver miniaturization in implantable medical devices and other WPT systems.

References

1. **Pendry JB, Holden AJ, Robbins DJ and Stewart WJ** (1999) Magnetism from conductors and enhanced nonlinear phenomena. *IEEE Transactions on Microwave Theory and Techniques* **47**, 2075–2084.
2. **Martın F, Bonache J, Falcone FA, Sorolla M and Marqués R** (2003) Split ring resonator-based left-handed coplanar waveguide. *Applied Physics Letters* **83**, 4652–4654.
3. **Hashemi SM, Soleimani M and Tretyakov SA** (2013) Compact negative-epsilon stop-band structures based on double-layer chiral inclusions. *IET Microwaves, Antennas & Propagation* **7**, 621–629.
4. **Baena JD, Bonache J, Martin F, Sillero RM, Falcone F, Lopetegi T and Sorolla M** (2005) Equivalent-circuit models for split-ring resonators and complementary split-ring resonators coupled to planar transmission lines. *IEEE Transactions on Microwave Theory and Techniques* **53**, 1451–1461.
5. **Baena JD, Marqués R, Medina F and Martel J** (2004) Artificial magnetic metamaterial design by using spiral resonators. *Physical Review B* **69**, 014402.
6. **Alici KB, Bilotti F, Vegni L and Ozbay E** (2007) Miniaturized negative permeability materials. *Applied Physics Letters* **91**, 071121.
7. **Bilotti F, Toscano A and Vegni L** (2007) Design of spiral and multiple split-ring resonators for the realization of miniaturized metamaterial samples. *IEEE Transactions on Antennas and Propagation* **55**, 2258–2267.
8. **Marqués R, Mesa F, Martel J and Medina F** (2003) Comparative analysis of edge-and broadside-coupled split ring resonators for metamaterial design-theory and experiments. *IEEE Transactions on Antennas and Propagation* **51**, 2572–2581.
9. **Ekmekci E and Turhan-Sayan G** (2008) Reducing the electrical size of magnetic metamaterial resonators by geometrical modifications: a comparative study for single-sided and double-sided multiple SRR, spiral and U-spiral resonators. In 2008 IEEE Antennas and Propagation Society International Symposium. IEEE. pp. 1–4.
10. **Aznar F, Gil M, Bonache J, Garcia-Garcia J and Martin F** (2007) Metamaterial transmission lines based on broad-side coupled spiral resonators. *Electronics Letters* **43**, 530–532.
11. **Aznar F, García-García J, Gil M, Bonache J and Martin F** (2008) Strategies for the miniaturization of metamaterial resonators. *Microwave and Optical Technology Letters* **50**, 1263–1270.
12. **Wiltshire MCK, Shamonina E, Young IR and Solymar L** (2003) Dispersion characteristics of magneto-inductive waves: comparison between theory and experiment. *Electronics Letters* **39**, 215–217.
13. **Martinez-Iranzo U, Moradi B, Garcia-Garcia J, Arasa E and Alonso J** (2014) Miniaturization of microwave resonant particles by the utilization of embedded high dielectric constant paste. In 2014 44th European Microwave Conference. IEEE. pp. 1214–1217.
14. **Kurter C, Abrahams J and Anlage SM** (2010) Miniaturized superconducting metamaterials for radio frequencies. *Applied Physics Letters* **96**, 253504.
15. **Rodríguez ESG, RamRakhyani AK, Schurig D and Lazzi G** (2016) Compact low-frequency metamaterial design for wireless power transfer efficiency enhancement. *IEEE Transactions on Microwave Theory and Techniques* **64**, 1644–1654.
16. **Hao T, Stevens CJ and Edwards DJ** (2008) Reducing electrical size of metamaterial elements: simulations and experiments. *Electronics Letters* **44**, 864–866.
17. **Martin F** (2015) *Artificial Transmission Lines for RF and Microwave Applications*. Hoboken, New Jersey: John Wiley & Sons, Inc. .
18. **Aznar F, Gil M, Bonache J, Jelinek L, Baena JD, Marqués R and Martín F** (2008) Characterization of miniaturized metamaterial resonators coupled to planar transmission lines through parameter extraction. *Journal of Applied Physics* **104**, 114501.
19. **Benkhaoua L, Benhabiles MT, Mouissat S and Riabi ML** (2016) Miniaturized quasi-lumped resonator for dielectric characterization of liquid mixtures. *IEEE Sensors Journal* **16**, 1603–1610.
20. **Jolani F, Yu Y and Chen Z** (2014) A planar magnetically coupled resonant wireless power transfer system using printed spiral coils. *IEEE Antennas and Wireless Propagation Letters* **13**, 1648–1651.
21. **Huang HF and Li T** (2016) A spiral electrically small magnetic antenna with high radiation efficiency for wireless power transfer. *IEEE Antennas and Wireless Propagation Letters* **15**, 1495–1498.

https://doi.org/10.1017/S1759078719001259 Published online by Cambridge University Press



L. Benkhaoua received the degree of Licence in Electronic, and Master in Electronic in 2010 and 2012, respectively, and received his Ph.D. degree in microwaves and telecommunications in 2016 at the Laboratory of Electromagnetism from University Frères Mentouri de Constantine, Algeria. He is currently a Senior Lecturer with the University 08 mai 1945 Guelma, Algeria. His research interest includes metamaterials, development of passive microwave devices and sensors.



S. Mouissat obtained the degree of Ingénieur en Electronique and Magister en Electronique in 1998 and 2000, respectively, both from University Frères Mentouri de Constantine, Algeria, where he is a teacher now. His main research areas are plasma science and printed circuit design.



M. T. Benhabiles obtained the degree of Ingénieur Civil Electricien from Université Catholique de Louvain, Belgium in 1982, Magister and Ph.D. in electronics from University Frères Mentouri de Constantine, Algeria, respectively, in 1995 and 2003, where he is currently a teaching Professor. His main research area is the numerical modeling of passive microwave devices.



M. L. Riabi received the degree of Ingénieur en Electronique from Ecole Polytechnique, Algeria, in 1979, and the Ph.D. degree in Microwave from Université de Toulouse, France, in 1992. He is currently a teaching Professor at University Frères Mentouri de Constantine, Algeria. His research interests are microwave passive devices. Pr Riabi is the chairman of the Laboratory of Electromagnetism and Telecommunication at University Frères Mentouri.

https://doi.org/10.1017/S1759078719001259 Published online by Cambridge University Press